Supplementary Information for

Quantifying Assets for the Geopolitics of Climate Change Mitigation

Contents

Supplementary Figures

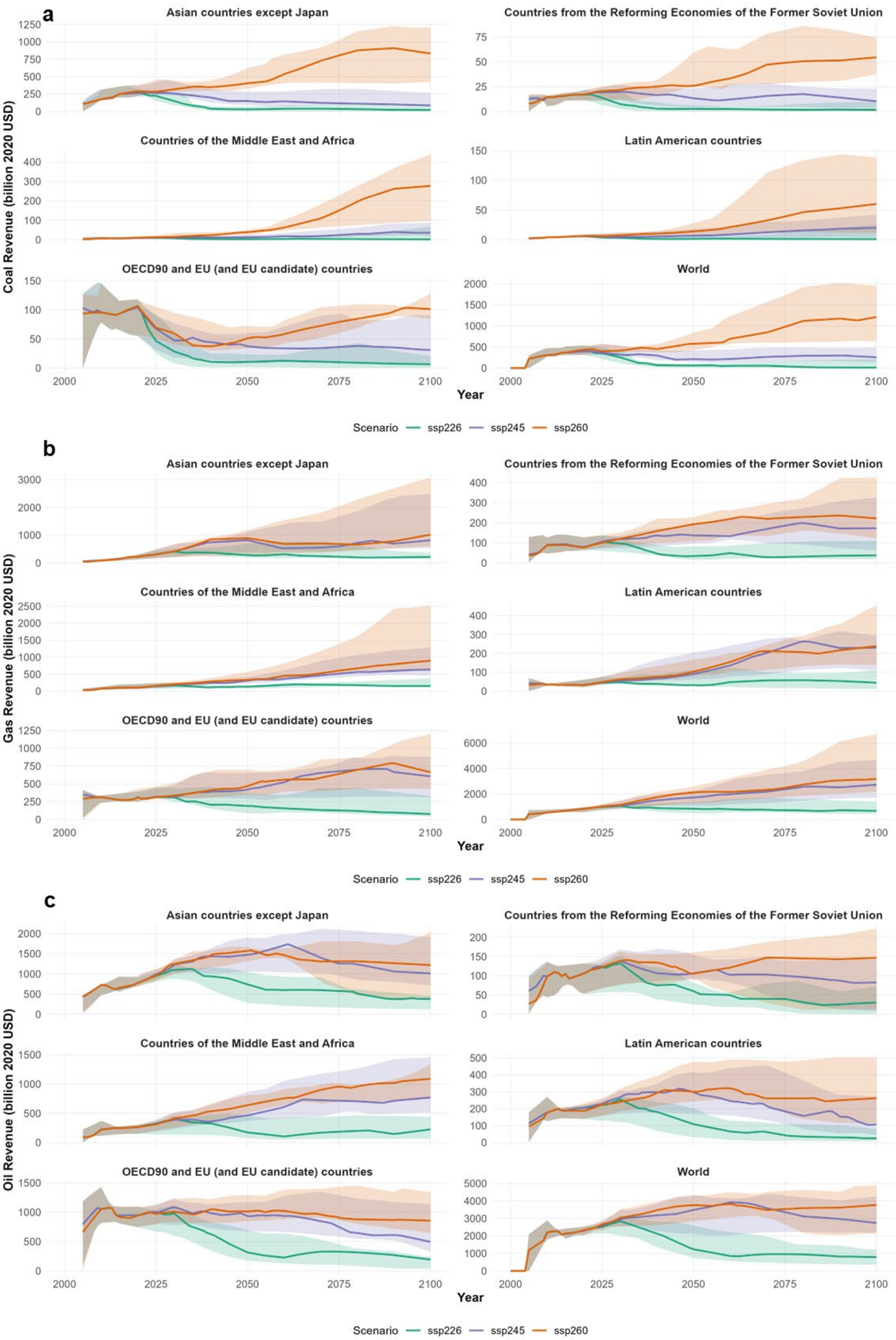

Supplementary Fig. 1 Fossil fuel revenues in AR6 R5 regions under two mitigation scenarios and the baseline. (a) Coal, (b) Gas, and (c) Oil revenues. Lines represent the multi-model median, and shaded areas indicate the 66.7% confidence interval across models.

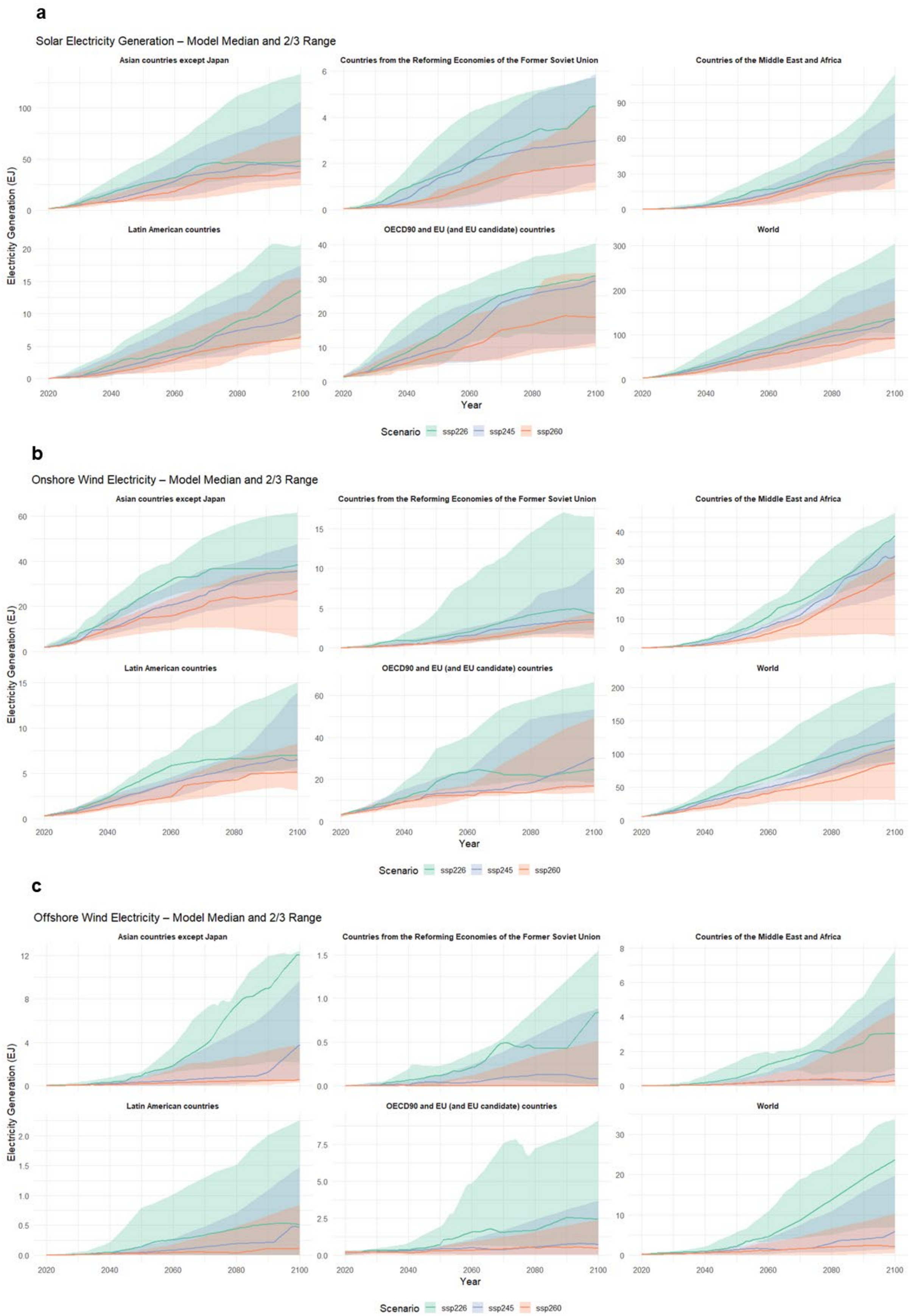

Supplementary Fig. 2 Renewable electricity generation in AR6 R5 regions under two mitigation scenarios and the baseline. (a) Solar, (b) Onshore wind, and (c) Offshore wind generation. Lines represent the multi-model median, and shaded areas indicate the 66.7% confidence interval across models.

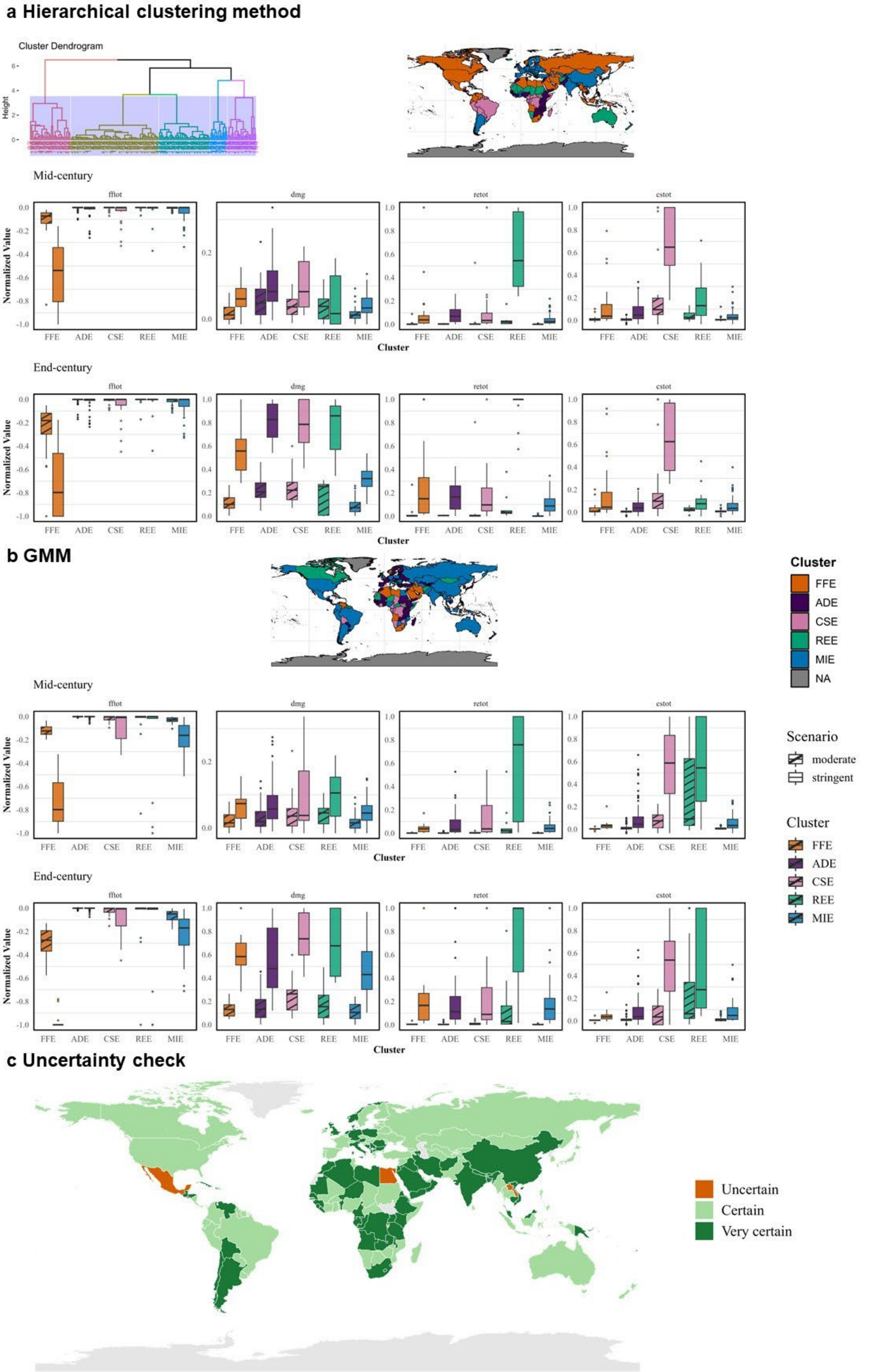
a Hierarchical clustering method
Cluster Dendrogram
Height
Mid-century
fftot
dmg
retot
cstot
Normalized Value
Cluster
End-century
b GMM
Cluster
FFE
ADE
CSE
REE
MIE
NA
Scenario
moderate
stringent
c Uncertainty check
Uncertain
Certain
Very certain

25

Supplementary Fig. 3 Clustering results from alternative methods. (a) Hierarchical clustering, (b) Gaussian Mixture Model (GMM), and (c) Uncertainty check. In panel (c), clustering uncertainty is categorized as follows: Uncertain—all three methods assign different clusters; Certain—two methods agree, one differs; Very certain—all three methods agree. Among 172 countries, 4 are identified as uncertain (Egypt, Laos, Mexico, and Samoa), 79 as very certain, and 89 as certain.

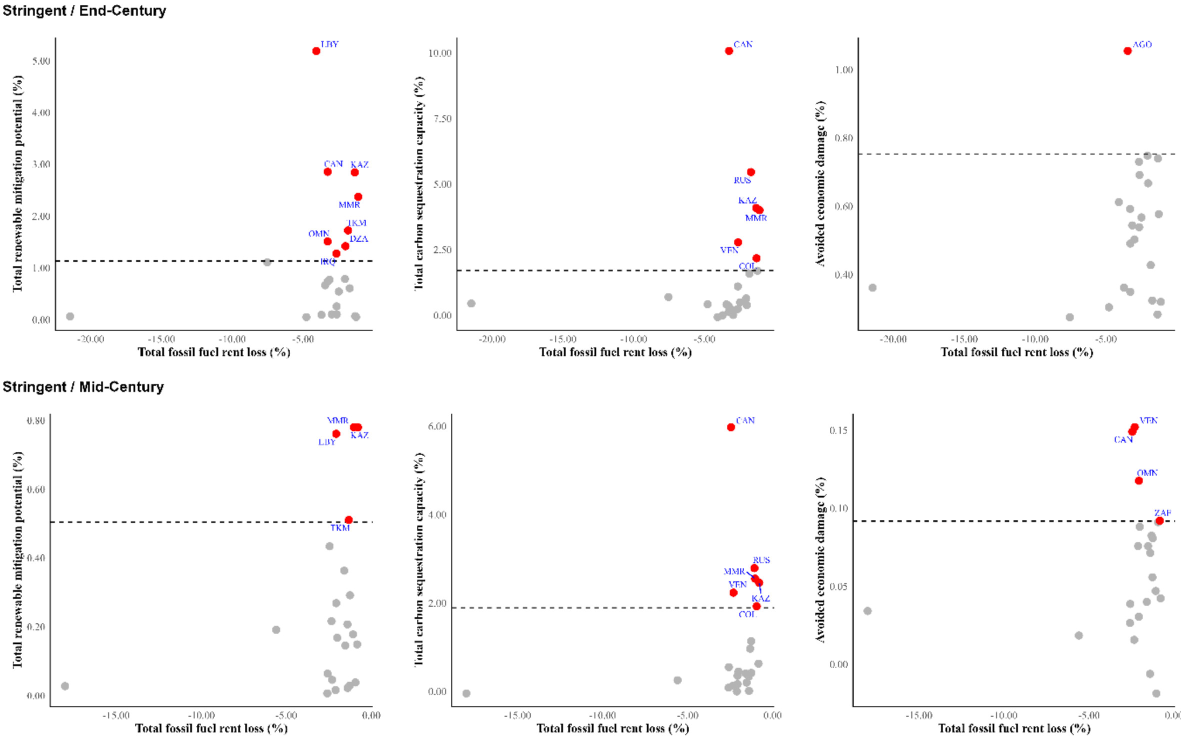

Supplementary Fig. 4 Scatter plots compare total fossil fuel rent losses (x-axis) with three key mitigation assets (y-axis): total renewable energy mitigation potential, total carbon sequestration capacity, and avoided economic damage, all expressed as percentages of each country's discounted cumulative GDP. The top row presents results for the stringent mitigation scenario by end-century, and the bottom row shows mid-century projections under the same scenario. The dashed horizontal lines represent the upper quartile (75th percentile) of the global distribution for each asset with all clusters included. Countries exceeding this threshold are highlighted in red, indicating stronger mitigation opportunities relative to fossil fuel losses within the FFE cluster.

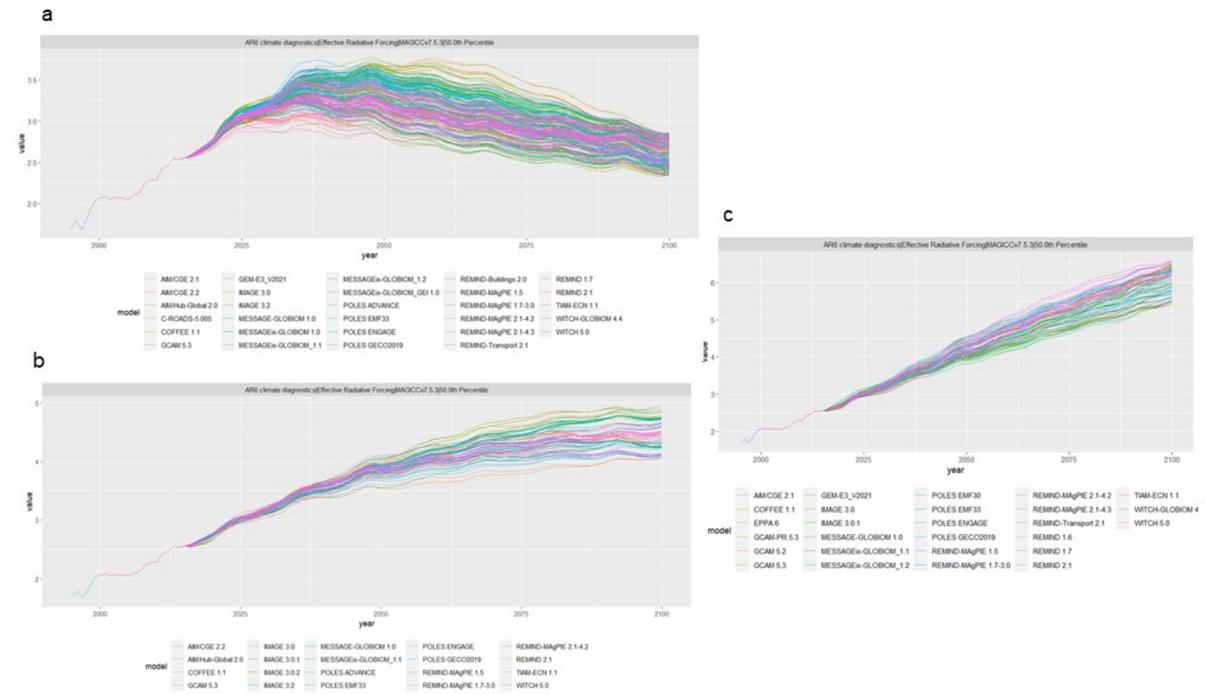

Supplementary Fig. 5 Selection of SSP2 scenarios from the AR6 database. Scenarios are filtered based on global median forcing values that fall within ±10% of target forcing levels: (a) 2.6, (b) 4.5, and (c) 6.0 W/m², respectively. The figure presents all IAMs that meet the criteria for each scenario; however, only IAMs common across all three scenarios are retained for the subsequent analysis.

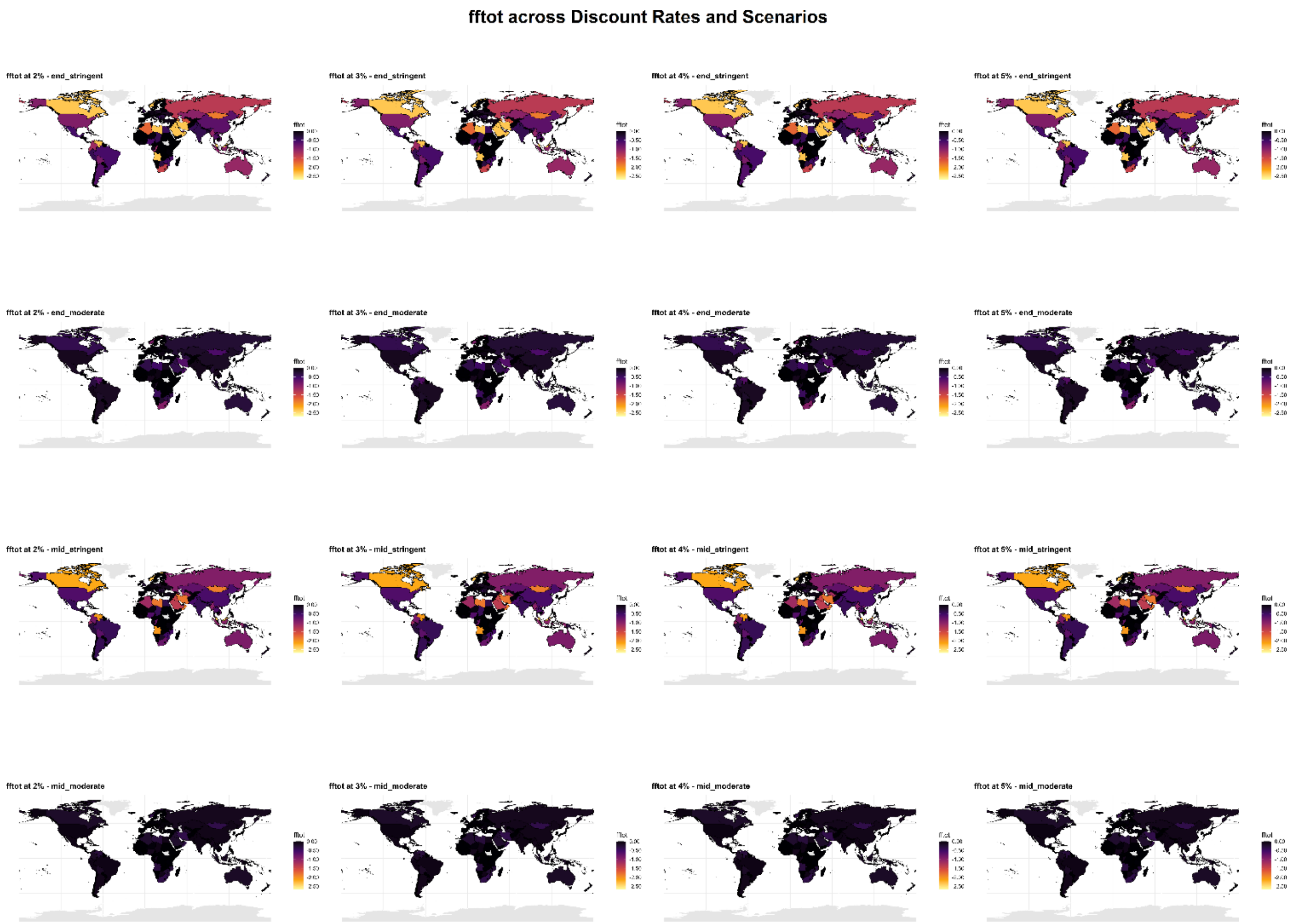

Supplementary Fig. 6.1 Sensitivity analysis for total fossil fuel rent loss (fftot) across discount rates. This figure displays total fossil fuel rent loss (fftot, unit: % of cumulative GDP) at discount rates of 2%, 3%, 4%, and 5%, under two mitigation scenarios (stringent and moderate) and two time periods (mid- and end-century).

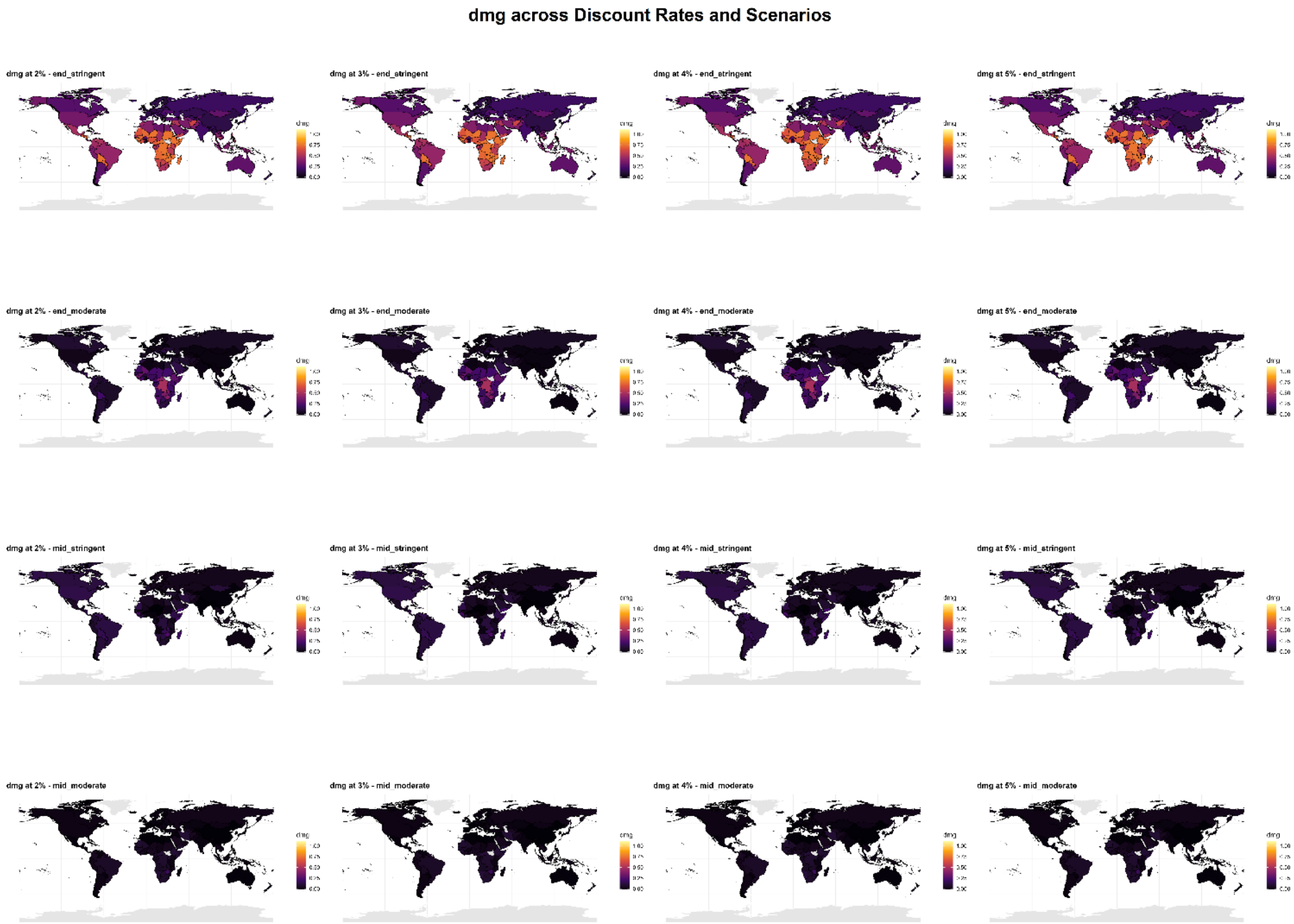

Supplementary Fig. 6.2 Sensitivity analysis for avoided economic damage (dmg) across discount rates. This figure displays avoided economic damage (dmg, unit: % of cumulative GDP) at discount rates of 2%, 3%, 4%, and 5%, under two mitigation scenarios (stringent and moderate) and two time periods (mid- and end-century).

Supplementary Fig. 6.3 Sensitivity analysis for total renewable mitigation potential (retot) across discount rates. This figure displays total renewable mitigation potential (retot, unit: % of cumulative GDP) at discount rates of 2%, 3%, 4%, and 5%, under two mitigation scenarios (stringent and moderate) and two time periods (mid- and end-century).

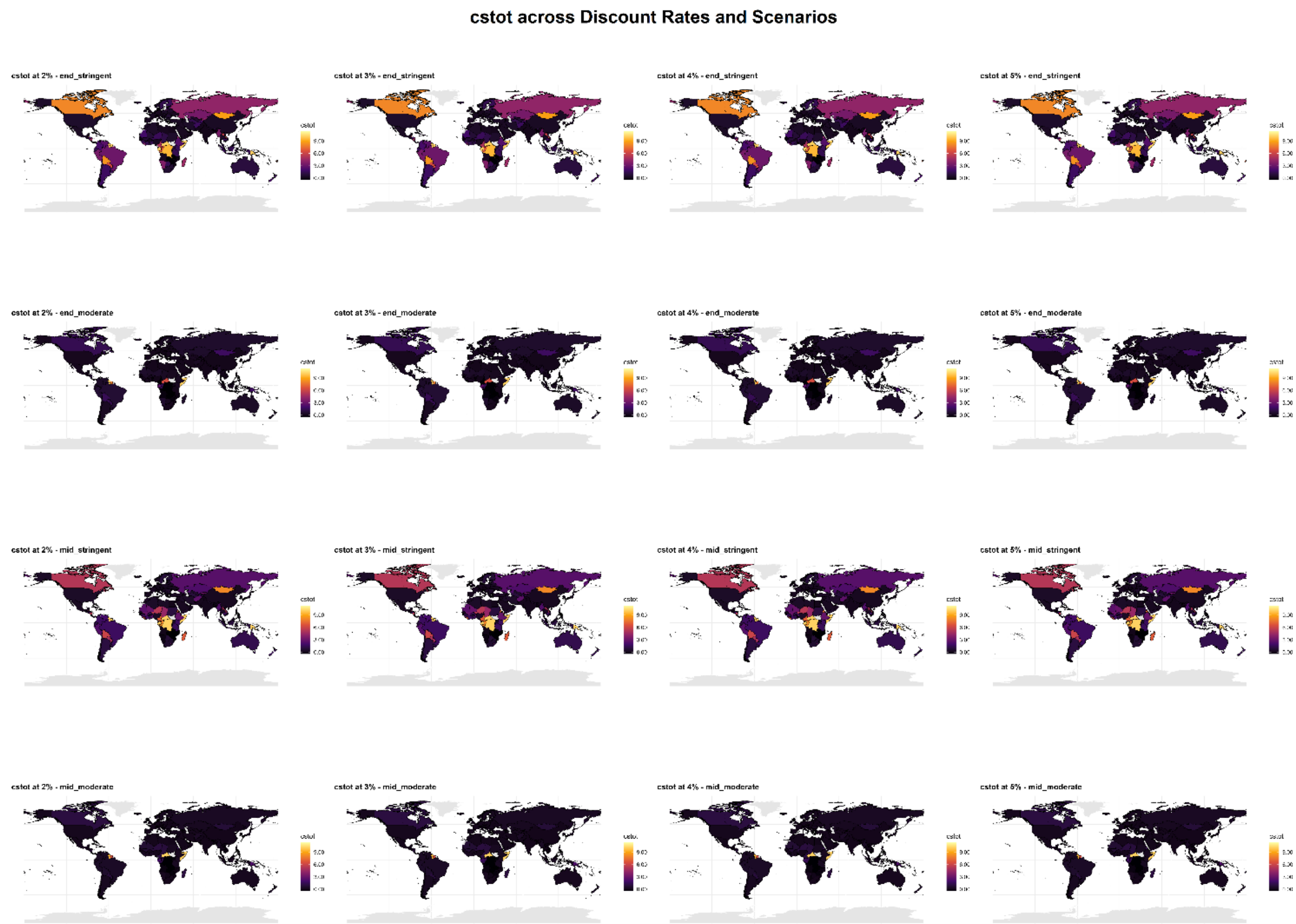

Supplementary Fig. 6.4 Sensitivity analysis for total carbon sequestration capacity (cstot) across discount rates. This figure displays total carbon sequestration capacity (cstot, unit: % of cumulative GDP) at discount rates of 2%, 3%, 4%, and 5%, under two mitigation scenarios (stringent and moderate) and two time periods (mid- and end-century).

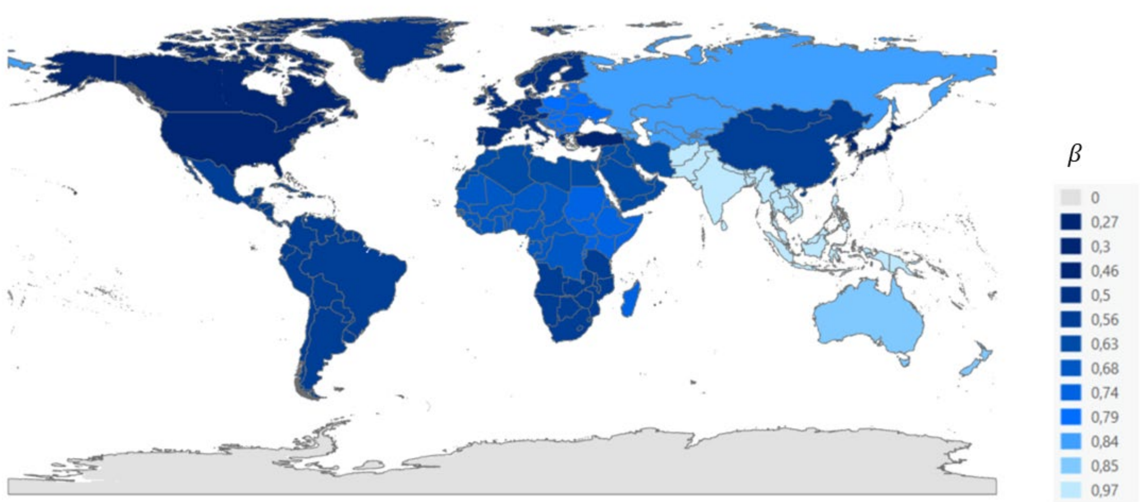

Supplementary Fig. 7 Region-specific coefficient β for converting floor area to roof area.

Supplementary Tables

Supplementary Table 1 Five most similar countries for each country based on distance-based similarity analysis. Similarity coefficient is calculated based on detailed sub-dimensional factors, including fossil fuel rent losses (coal, gas, oil), avoided economic damage, mitigation potential from solar and wind energy generation, and natural and managed carbon sequestration capacities.

ISO3	Top1	Top2	Top3	Top4	Top5
AFG	NER (0.58)	ERI (0.55)	MLI (0.52)	MRT (0.5)	TCD (0.49)
AGO	IRQ (0.44)	SAU (0.44)	ECU (0.43)	KWT (0.42)	COG (0.41)
ALB	HRV (0.82)	ITA (0.8)	HUN (0.8)	SVK (0.79)	SVN (0.79)
ARE	THA (0.75)	ALB (0.7)	MEX (0.7)	USA (0.69)	DNK (0.67)
ARG	USA (0.65)	NZL (0.63)	EGY (0.62)	ISR (0.62)	PER (0.61)
ARM	EST (0.74)	LTU (0.73)	SVK (0.73)	BLR (0.73)	FIN (0.73)
AUS	KAZ (0.48)	CHN (0.46)	BWA (0.46)	IDN (0.46)	ZAF (0.46)
AUT	ITA (0.91)	CHE (0.9)	ESP (0.89)	BEL (0.89)	FRA (0.87)
AZE	IRN (0.7)	DZA (0.67)	OMN (0.6)	QAT (0.54)	TKM (0.53)
BDI	RWA (0.59)	BEN (0.56)	SWZ (0.55)	YEM (0.52)	NPL (0.52)
BEL	LUX (0.92)	CHE (0.91)	ESP (0.91)	FRA (0.9)	SVK (0.9)
BEN	RWA (0.74)	TZA (0.72)	KEN (0.72)	SWZ (0.71)	MWI (0.7)
BFA	TJK (0.75)	TGO (0.71)	KEN (0.69)	KGZ (0.68)	YEM (0.65)
BGD	TGO (0.64)	PAK (0.63)	TJK (0.63)	MDA (0.62)	UZB (0.62)
BGR	MKD (0.77)	BIH (0.74)	MNE (0.71)	IND (0.69)	CHN (0.67)
BHS	URY (0.72)	CUB (0.66)	WSM (0.66)	MUS (0.65)	IRL (0.64)
BIH	BGR (0.74)	CHN (0.71)	MNE (0.68)	MKD (0.66)	SRB (0.65)
BLR	CHL (0.87)	SVK (0.87)	CHE (0.87)	ESP (0.86)	FRA (0.85)
BLZ	PRY (0.66)	CMR (0.65)	NIC (0.57)	HND (0.56)	KHM (0.55)
BOL	PER (0.48)	PRY (0.48)	BLZ (0.45)	BRA (0.44)	GAB (0.44)
BRA	PER (0.7)	THA (0.65)	MEX (0.65)	PAN (0.63)	USA (0.63)
BRN	TTO (0.47)	NOR (0.44)	IRN (0.4)	OMN (0.4)	QAT (0.39)
BTN	NPL (0.48)	KGZ (0.44)	TJK (0.44)	SWZ (0.42)	BFA (0.42)
BWA	COL (0.54)	CHN (0.51)	BIH (0.51)	BGR (0.51)	ZAF (0.51)
CAF	COD (0.37)	MDG (0.36)	BLZ (0.34)	GAB (0.34)	CMR (0.34)
CAN	LBY (0.48)	MYS (0.43)	VEN (0.43)	NOR (0.42)	SAU (0.41)
CHE	ESP (0.93)	FRA (0.91)	BEL (0.91)	AUT (0.9)	SVK (0.9)
CHL	HKG (0.87)	BLR (0.87)	SWE (0.87)	KOR (0.86)	FIN (0.86)
CHN	BIH (0.71)	BGR (0.67)	IDN (0.63)	IND (0.6)	MKD (0.58)
CIV	SYR (0.82)	GTM (0.79)	JOR (0.79)	GMB (0.77)	MAR (0.77)
CMR	BLZ (0.65)	LBR (0.61)	BEN (0.59)	TZA (0.57)	CIV (0.56)
COD	MDG (0.42)	ETH (0.38)	BLZ (0.38)	CMR (0.37)	CAF (0.37)
COG	GAB (0.52)	NIC (0.51)	PRY (0.51)	BLZ (0.5)	BRA (0.46)
COL	CHN (0.58)	IDN (0.57)	BWA (0.54)	BIH (0.53)	BGR (0.53)
COM	SLV (0.87)	GTM (0.79)	CRI (0.79)	HTI (0.78)	PSE (0.76)
CPV	PRI (0.9)	CYP (0.89)	PRT (0.89)	JPN (0.89)	PYF (0.87)
CRI	PAN (0.87)	HTI (0.86)	LKA (0.84)	DOM (0.82)	JAM (0.81)
CUB	WSM (0.73)	SWE (0.72)	URY (0.72)	CPV (0.71)	CRI (0.7)
CYP	JPN (0.93)	PRT (0.93)	PRI (0.9)	CPV (0.89)	PYF (0.88)
CZE	POL (0.88)	DEU (0.84)	SVN (0.8)	UKR (0.8)	GRC (0.79)

DEU	CHE (0.86)	ESP (0.86)	FRA (0.85)	SVN (0.85)	SVK (0.85)
DJI	SEN (0.77)	UZB (0.73)	YEM (0.72)	MDA (0.71)	TUN (0.69)
DNK	IRL (0.82)	MUS (0.81)	KOR (0.81)	GBR (0.79)	CHL (0.79)
DOM	LBN (0.91)	LKA (0.9)	JAM (0.89)	PRT (0.87)	CYP (0.87)
DZA	AZE (0.67)	IRN (0.62)	OMN (0.61)	TKM (0.54)	USA (0.54)
ECU	KWT (0.67)	SAU (0.65)	ARE (0.65)	THA (0.64)	USA (0.6)
EGY	ISR (0.74)	MEX (0.73)	NGA (0.72)	TUN (0.7)	USA (0.7)
ERI	NER (0.65)	AFG (0.55)	MLI (0.53)	TCD (0.46)	MRT (0.45)
ESP	CHE (0.93)	SVK (0.92)	FRA (0.91)	BEL (0.91)	ITA (0.9)
EST	LTU (0.88)	AUT (0.85)	ESP (0.85)	ITA (0.84)	BLR (0.84)
ETH	UGA (0.68)	MDG (0.67)	SLE (0.65)	MWI (0.62)	KEN (0.6)
FIN	SWE (0.91)	CHL (0.86)	BLR (0.85)	CPV (0.84)	PRI (0.83)
FJI	VUT (0.73)	GEO (0.58)	LVA (0.58)	BRA (0.57)	EST (0.57)
FRA	CHE (0.91)	ESP (0.91)	BEL (0.9)	LUX (0.89)	AUT (0.87)
GAB	PRY (0.61)	NIC (0.58)	BLZ (0.53)	COG (0.52)	PNG (0.51)
GBR	FRA (0.79)	DNK (0.79)	NLD (0.79)	CHE (0.78)	IRL (0.78)
GEO	LVA (0.81)	EST (0.76)	LTU (0.74)	AUT (0.73)	ARM (0.72)
GHA	LTU (0.79)	LUX (0.78)	SVK (0.77)	HRV (0.77)	FRA (0.75)
GIN	CIV (0.75)	GTM (0.74)	SLE (0.71)	SYR (0.71)	COM (0.69)
GMB	SYR (0.83)	JOR (0.83)	MAR (0.83)	PSE (0.82)	SLV (0.79)
GNB	SDN (0.58)	DJI (0.54)	MRT (0.53)	NAM (0.52)	TLS (0.52)
GNQ	CRI (0.8)	HTI (0.78)	PAN (0.76)	MAR (0.75)	LKA (0.74)
GRC	TUR (0.86)	CYP (0.84)	PRT (0.84)	JPN (0.83)	LBN (0.82)
GTM	SLV (0.8)	CIV (0.79)	COM (0.79)	SYR (0.77)	GMB (0.75)
GUY	SUR (0.7)	PNG (0.44)	FJI (0.39)	GAB (0.39)	VUT (0.38)
HKG	PYF (0.93)	NLD (0.88)	PRI (0.88)	CHE (0.87)	JPN (0.87)
HND	CIV (0.76)	GTM (0.72)	GNQ (0.7)	SLV (0.7)	COM (0.7)
HRV	SVK (0.89)	ESP (0.88)	BEL (0.87)	SVN (0.87)	ITA (0.85)
HTI	CRI (0.86)	PAN (0.85)	LKA (0.83)	JAM (0.82)	PSE (0.82)
HUN	SVN (0.86)	HRV (0.85)	UKR (0.82)	BEL (0.81)	ALB (0.8)
IDN	CHN (0.63)	COL (0.57)	BIH (0.56)	BGR (0.56)	IND (0.51)
IND	MKD (0.76)	MNE (0.74)	BGR (0.69)	POL (0.68)	ROU (0.67)
IRL	CHL (0.86)	KOR (0.85)	ESP (0.83)	DNK (0.82)	FRA (0.82)
IRN	AZE (0.7)	OMN (0.69)	DZA (0.62)	QAT (0.61)	TTO (0.59)
IRQ	SAU (0.65)	KWT (0.59)	ECU (0.55)	MYS (0.53)	VEN (0.53)
ISL	TLS (0.52)	MUS (0.5)	DNK (0.49)	TUN (0.49)	NZL (0.49)
ISR	MEX (0.75)	PHL (0.75)	LBN (0.74)	HTI (0.74)	EGY (0.74)
ITA	JPN (0.91)	AUT (0.91)	CHE (0.9)	BEL (0.9)	ESP (0.9)
JAM	DOM (0.89)	PAN (0.87)	LKA (0.87)	LBN (0.85)	CPV (0.85)
JOR	SYR (0.9)	GMB (0.83)	MAR (0.81)	CIV (0.79)	TUN (0.74)
JPN	CYP (0.93)	PYF (0.93)	PRI (0.92)	PRT (0.91)	ITA (0.91)
KAZ	AUS (0.48)	CHN (0.46)	VNM (0.43)	BIH (0.43)	BWA (0.43)
KEN	TZA (0.75)	MWI (0.73)	SWZ (0.72)	YEM (0.72)	BEN (0.72)
KGZ	BFA (0.68)	TJK (0.67)	TGO (0.63)	NPL (0.61)	YEM (0.6)
KHM	TZA (0.71)	SEN (0.69)	KEN (0.69)	SLE (0.67)	DJI (0.67)
KOR	PYF (0.89)	PRI (0.88)	JPN (0.88)	PRT (0.88)	HKG (0.87)
KWT	SAU (0.8)	ECU (0.67)	MYS (0.6)	VEN (0.6)	IRQ (0.59)
LAO	SRB (0.41)	MNE (0.39)	BIH (0.38)	ZWE (0.37)	IND (0.37)
LBN	DOM (0.91)	LKA (0.9)	PRT (0.89)	CYP (0.88)	JPN (0.86)

LBR	CMR (0.61)	BEN (0.55)	GIN (0.52)	CIV (0.52)	RWA (0.51)
LBY	SAU (0.51)	MYS (0.49)	CAN (0.48)	KWT (0.47)	IRQ (0.46)
LKA	LBN (0.9)	DOM (0.9)	JAM (0.87)	PAN (0.85)	PRT (0.85)
LSO	SLE (0.61)	TZA (0.59)	UGA (0.58)	ETH (0.57)	GIN (0.55)
LTU	ESP (0.89)	SVK (0.88)	EST (0.88)	CHE (0.87)	LUX (0.86)
LUX	BEL (0.92)	SVK (0.9)	FRA (0.89)	CHE (0.89)	ESP (0.88)
LVA	GEO (0.81)	EST (0.8)	LTU (0.78)	AUT (0.76)	ESP (0.73)
MAR	LKA (0.85)	GMB (0.83)	TUN (0.82)	SYR (0.81)	JOR (0.81)
MDA	UZB (0.79)	HUN (0.78)	HRV (0.76)	SEN (0.75)	GHA (0.73)
MDG	ETH (0.67)	SLE (0.54)	LSO (0.54)	UGA (0.53)	KEN (0.51)
MEX	THA (0.78)	ISR (0.75)	PHL (0.74)	USA (0.74)	EGY (0.73)
MKD	MNE (0.78)	BGR (0.77)	IND (0.76)	ROU (0.69)	POL (0.68)
MLI	NER (0.63)	TCD (0.58)	ERI (0.53)	AFG (0.52)	MRT (0.5)
MMR	TKM (0.6)	PAK (0.48)	DZA (0.48)	AZE (0.48)	BGD (0.46)
MNE	MKD (0.78)	IND (0.74)	BGR (0.71)	BIH (0.68)	ROU (0.62)
MNG	AUS (0.36)	MOZ (0.34)	ZAF (0.33)	KAZ (0.33)	BWA (0.32)
MOZ	ZAF (0.48)	ZWE (0.45)	BWA (0.44)	SRB (0.44)	BIH (0.4)
MRT	NAM (0.61)	GNB (0.53)	SDN (0.51)	TCD (0.51)	AFG (0.5)
MUS	KOR (0.85)	CYP (0.83)	PRT (0.82)	JPN (0.82)	IRL (0.81)
MWI	RWA (0.75)	KEN (0.73)	TZA (0.73)	SLE (0.72)	SWZ (0.7)
MYS	KWT (0.6)	VEN (0.6)	SAU (0.6)	ECU (0.54)	IRQ (0.53)
NAM	MRT (0.61)	SDN (0.53)	GNB (0.52)	DJI (0.48)	BHS (0.47)
NCL	SLB (0.45)	URY (0.45)	CUB (0.44)	BHS (0.42)	WSM (0.42)
NER	ERI (0.65)	MLI (0.63)	AFG (0.58)	TCD (0.52)	MRT (0.46)
NGA	EGY (0.72)	SYR (0.69)	JOR (0.68)	CIV (0.67)	MEX (0.66)
NIC	PRY (0.66)	GAB (0.58)	BLZ (0.57)	CMR (0.54)	HND (0.53)
NLD	HKG (0.88)	PYF (0.88)	ITA (0.88)	CHE (0.87)	JPN (0.87)
NOR	TTO (0.61)	OMN (0.55)	IRN (0.5)	DZA (0.47)	AZE (0.47)
NPL	KGZ (0.61)	TJK (0.6)	SWZ (0.58)	YEM (0.55)	BFA (0.54)
NZL	SWE (0.71)	IRL (0.7)	DNK (0.7)	FIN (0.7)	CHL (0.69)
OMN	IRN (0.69)	DZA (0.61)	AZE (0.6)	TTO (0.59)	NOR (0.55)
PAK	BGD (0.63)	YEM (0.61)	EGY (0.6)	DJI (0.59)	SEN (0.59)
PAN	JAM (0.87)	CRI (0.87)	LKA (0.85)	HTI (0.85)	DOM (0.84)
PER	BRA (0.7)	ISR (0.64)	PAN (0.63)	MEX (0.63)	JAM (0.62)
PHL	TUR (0.81)	MAR (0.78)	LKA (0.78)	LBN (0.77)	HTI (0.77)
PNG	FJI (0.54)	BLZ (0.53)	PRY (0.52)	GAB (0.51)	VUT (0.5)
POL	CZE (0.88)	DEU (0.78)	UKR (0.77)	SVN (0.75)	GRC (0.73)
PRI	JPN (0.92)	PYF (0.91)	CPV (0.9)	CYP (0.9)	PRT (0.88)
PRT	CYP (0.93)	JPN (0.91)	LBN (0.89)	CPV (0.89)	PRI (0.88)
PRY	BLZ (0.66)	NIC (0.66)	GAB (0.61)	HND (0.56)	CMR (0.55)
PSE	GMB (0.82)	HTI (0.82)	SLV (0.81)	TUN (0.81)	MAR (0.8)
PYF	HKG (0.93)	JPN (0.93)	PRI (0.91)	ITA (0.9)	KOR (0.89)
QAT	IRN (0.61)	AZE (0.54)	OMN (0.54)	TTO (0.52)	TKM (0.51)
ROU	UKR (0.77)	HUN (0.76)	SVN (0.74)	POL (0.73)	CZE (0.73)
RUS	AZE (0.48)	DZA (0.48)	USA (0.46)	ARG (0.46)	PER (0.46)
RWA	MWI (0.75)	BEN (0.74)	TZA (0.69)	SWZ (0.69)	KEN (0.69)
SAU	KWT (0.8)	ECU (0.65)	IRQ (0.65)	MYS (0.6)	VEN (0.59)
SDN	DJI (0.58)	GNB (0.58)	KEN (0.56)	YEM (0.55)	PAK (0.54)
SEN	DJI (0.77)	MDA (0.75)	YEM (0.74)	UZB (0.73)	JOR (0.72)

SLB	NCL (0.45)	ZMB (0.41)	URY (0.37)	CUB (0.37)	WSM (0.36)
SLE	TZA (0.74)	MWI (0.72)	GIN (0.71)	KEN (0.68)	UGA (0.68)
SLV	COM (0.87)	HTI (0.81)	PSE (0.81)	GTM (0.8)	MAR (0.79)
SOM	CAF (0.31)	ERI (0.3)	COD (0.3)	NER (0.28)	MDG (0.28)
SRB	BIH (0.65)	CHN (0.56)	MNE (0.55)	BGR (0.54)	MKD (0.51)
SUR	GUY (0.7)	PNG (0.45)	GAB (0.44)	PRY (0.4)	FJI (0.4)
SVK	ESP (0.92)	CHE (0.9)	BEL (0.9)	LUX (0.9)	HRV (0.89)
SVN	BEL (0.88)	HRV (0.87)	SVK (0.86)	ESP (0.86)	ITA (0.86)
SWE	FIN (0.91)	CHL (0.87)	BLR (0.84)	CPV (0.82)	PRI (0.82)
SWZ	KEN (0.72)	BEN (0.71)	MWI (0.7)	RWA (0.69)	YEM (0.67)
SYR	JOR (0.9)	GMB (0.83)	CIV (0.82)	MAR (0.81)	SLV (0.78)
TCD	MLI (0.58)	NER (0.52)	MRT (0.51)	GNB (0.5)	AFG (0.49)
TGO	MDA (0.73)	GHA (0.73)	BFA (0.71)	UZB (0.7)	TJK (0.7)
THA	MEX (0.78)	USA (0.77)	ARE (0.75)	ALB (0.72)	VNM (0.69)
TJK	BFA (0.75)	TGO (0.7)	YEM (0.68)	KGZ (0.67)	KEN (0.67)
TKM	MMR (0.6)	DZA (0.54)	AZE (0.53)	IRN (0.52)	QAT (0.51)
TLS	TUN (0.6)	PSE (0.57)	BHS (0.57)	DJI (0.56)	MUS (0.56)
TTO	NOR (0.61)	IRN (0.59)	OMN (0.59)	AZE (0.53)	QAT (0.52)
TUN	MAR (0.82)	PSE (0.81)	GMB (0.78)	LKA (0.78)	LBN (0.75)
TUR	GRC (0.86)	DOM (0.84)	LBN (0.84)	LKA (0.84)	PRT (0.82)
TZA	KEN (0.75)	SLE (0.74)	MWI (0.73)	BEN (0.72)	KHM (0.71)
UGA	MWI (0.7)	ETH (0.68)	SLE (0.68)	KEN (0.66)	TZA (0.65)
UKR	SVN (0.84)	GRC (0.82)	HUN (0.82)	TUR (0.81)	CZE (0.8)
URY	WSM (0.76)	BHS (0.72)	CUB (0.72)	SWE (0.68)	NZL (0.67)
USA	THA (0.77)	MEX (0.74)	EGY (0.7)	ARE (0.69)	ISR (0.66)
UZB	MDA (0.79)	HRV (0.74)	SEN (0.73)	HUN (0.73)	UKR (0.73)
VEN	MYS (0.6)	KWT (0.6)	SAU (0.59)	ECU (0.56)	IRQ (0.53)
VNM	THA (0.69)	USA (0.65)	IND (0.63)	ROU (0.63)	ALB (0.62)
VUT	FJI (0.73)	GEO (0.6)	EST (0.59)	LVA (0.59)	JAM (0.58)
WSM	URY (0.76)	SWE (0.73)	CUB (0.73)	JAM (0.71)	PAN (0.71)
YEM	SEN (0.74)	DJI (0.72)	KEN (0.72)	MDA (0.69)	TJK (0.68)
ZAF	BWA (0.51)	SRB (0.51)	MOZ (0.48)	BIH (0.46)	AUS (0.46)
ZMB	UGA (0.5)	TZA (0.47)	LSO (0.47)	SLE (0.47)	ETH (0.46)
ZWE	MOZ (0.45)	SRB (0.43)	ZAF (0.42)	BWA (0.4)	BIH (0.38)

Supplementary Table 2 CMIP6 General Circulation Models (GCMs) employed in this study.

GCM	**RCP26 (SSP126)**	**RCP45 (SSP245)**	**RCP60 (SSP460)**
CanESM5	×	×	×
CanESM5-1	×	×	×
FGOALS-g3	×	×	×
IPSL-CM6A-LR	×	×	×
MIROC6	×	×	×
MRI-ESM2-0	×	×	×

Supplementary Table 3 The land suitability factors of different land or sea pixel types, based on Gernaat et al.'s study[1].

Land/Sea pixel type	**LSF (Utility PV, %)**	**LSF (Onshore Wind, %)**	**LSF (Offshore wind, %)**
Forest	0	10	-
Tropical forest	0	0	
Barren land	5	100	-
Shrubland	1	50	-
Tropical shrubland	0	0	
Extensive grassland	5	80	-
grassland	1	80	-
Cropland	1	70	-
Biofuel land	0	70	
Urban area	0	0	-
Pixel with urban fraction > 90%	0	0	-
Average elevation > 2km	0	0	-
Average slope > 5 degree	0	0	-
Environmental protected area	0	0	-
Marine protected area	-	-	0
Shipping lanes	-	-	85
Exclusive economic zone (EEZ)	-	-	100
Sea area outside the EEZ	-	-	0
Sea area covered with permanent ice and snow	-	-	0
See depth > 1km	-	-	0

Supplementary Text

S1. Panel efficiency calculation

The photovoltaic (PV) panel efficiency at a given grid cell i and year t is calculated as:

$$\eta_{PV,i,t} = 17\% \times (1 + \gamma[T_{i,t} - T_{STC}])$$

Where $T_{i,t}$ is the PV cell temperature, $T_{STC} = 25°\mathrm{C}$ represents the standard condition, and γ is the temperature coefficient of efficiency, reflecting the rate at which efficiency decreases with increasing temperature, which is -0.005 $°\mathrm{C}^{-1}$[2].

Then, The PV cell temperature $T_{i,t}$ is estimated as a function of ambient environmental conditions using the following empirical equation:

$$T_{i,t} = c_1 + c_2 \cdot tas_{i,t} + c_3 \cdot rsds_{i,t} + c_4 \cdot vws_{i,t}$$

Where $tas_{i,t}$, $rsds_{i,t}$, $vws_{i,t}$ are ambient temperature, solar irradiation, wind speed (10m height), respectively, which can be derived from climate model datasets. The coefficients used in the temperature model are: c_1=4.3°C, c_2=0.943, c_3=0.028°C $\mathrm{m}^2\,\mathrm{W}^{-1}$ and c_4=-1.528°C sm^{-1}[1,3].

S2. CF calculation method

To calculate the capacity factor (CF), a Weibull distribution function is employed to estimate the wind speed distribution over the course of a year. The probability of wind turbine operation within a specific wind speed range is determined using the cumulative Weibull distribution function:

$$P(v_c < v < v_f) = exp\,[-(v_c/c)^k] - exp\,[-(v_f/c)^k]$$

$$c = v \times (0.568{+}0.433/k)^{-\frac{1}{k}}$$

where $P(v_c < v < v_f)$ denotes the operation probability of a turbine; v_c is the cut in speed; v_f is the cut out speed; c and k are the Weibull scale parameter and shape parameter, respectively; In this study, the hub height is set as 100m and the wind speed at 100m height can be estimated according to the surface wind speed data from CMIP 6:

$$v{=}v_{ref} \times (H/H_{ref})^{\alpha}$$

Subsequently, CF is derived from the probability distribution functions of wind turbine operation[4],

$$CF = \frac{\exp\left(-\left(\frac{v_c}{c}\right)^k\right) - \exp\left(-\left(\frac{v_r}{c}\right)^k\right)}{\left(\frac{v_r}{c}\right)^k - \left(\frac{v_c}{c}\right)^k} - \exp\left(-\left(\frac{v_f}{c}\right)^k\right)$$

where v_c, v_r, and v_f denote the cut-in wind speed (4 m/s), rated wind speed (13 m/s), and cut-out wind speed (25 m/s), respectively. The parameter k is the shape factor of the Weibull distribution, set to k=2[1], while c is the scale factor, calculated from the mean wind speed v and the shape parameter k. Together, these parameters characterize the wind speed distribution, which forms the basis for estimating the capacity factor. This formulation integrates the probabilistic characteristics of wind speed distributions with turbine operating parameters, enabling the estimation of capacity factor (CF) as a measure of expected energy generation under varying wind conditions.

References

1 Gernaat, D. E. H. J. *et al.* Climate change impacts on renewable energy supply. *Nature Climate Change* **11**, 119-125 (2021). https://doi.org:10.1038/s41558-020-00949-9

2 Tonui, J. K. & Tripanagnostopoulos, Y. Performance improvement of PV/T solar collectors with natural air flow operation. *Solar Energy* **82**, 1-12 (2008). https://doi.org:https://doi.org/10.1016/j.solener.2007.06.004

3 Chenni, R., Makhlouf, M., Kerbache, T. & Bouzid, A. A detailed modeling method for photovoltaic cells. *Energy* **32**, 1724-1730 (2007). https://doi.org:https://doi.org/10.1016/j.energy.2006.12.006

4 Sasi, K. K. & Basu, S. On the Prediction of Capacity Factor and Selection of Size of Wind Electric Generators — a Study based on Indian Sites. *Wind Engineering* **21**, 73-88 (1997).